

Room-temperature polariton luminescence from a bulk GaN microcavity

R. Butté, G. Christmann, E. Felton, J.-F. Carlin, M. Mosca, M. Illegems, and N. Grandjean

École Polytechnique Fédérale de Lausanne (EPFL), Institute of Quantum Electronics and Photonics, CH-1015 Lausanne, Switzerland

(Received 4 October 2005; published 19 January 2006)

We report strong exciton-photon coupling at room temperature in a hybrid high quality bulk $3\lambda/2$ GaN cavity with a bottom lattice-matched AlInN/AlGaIn distributed Bragg reflector through angle-resolved polarized photoluminescence (PL). Coupling of the optically active free excitons (X_A , X_B , and X_C) to the cavity mode is demonstrated, with their contribution to the PL spectra varying with polarization. Under TE polarization, exciton oscillator strengths for X_A and X_B are about one order of magnitude larger than in bulk GaAs. Photoluminescence exhibits a strong bottleneck effect despite its thermal lineshape.

DOI: [10.1103/PhysRevB.73.033315](https://doi.org/10.1103/PhysRevB.73.033315)

PACS number(s): 78.67.-n, 71.36.+c, 78.20.Ci, 78.55.Cr

In the past decade, strong light-matter interaction in solid state systems has attracted much interest.^{1,2} To carry out such experiments, semiconductor microcavities (MCs) are among the most widely used as they allow tailoring of the strength of the interaction between the elementary excitations in semiconductors, namely excitons and cavity photons. Owing to their geometry, planar MCs (GaAs and II-VI based) containing either quantum wells² (QW-MCs) or a bulk cavity³ are prototypical systems to manipulate cavity polaritons (CPs)—the quasiparticles issued from the mixing of excitons and photons. A major aspect of CP physics is the demonstration of large nonlinearities, which has triggered an entire research field.⁴ Another consequence of the bosonic character of CPs when combined to their small density of states is the potential formation of dynamical Bose-Einstein condensates.⁵ Furthermore, MCs operating in the strong coupling regime (SCR) are promising candidates to investigate optoelectronics devices such as polariton light emitters⁶ or ultrafast micro-optical amplifiers.^{4,7}

However, structures operating at room temperature (RT) based on CP nonlinear phenomena (e.g., parametric amplification) are out of reach of GaAs MCs due to their small exciton binding energy, E_X^B . Indeed, the cutoff temperature of such effects scales linearly to E_X^B ,⁷ thereby limiting these phenomena in GaAs-based MCs to low cryogenic temperatures. In II-VI semiconductors, the larger E_X^B allows for the observation of nonlinearities up to 220 K in CdTe-based MCs. Nevertheless, II-VI materials have not proved viable for technological applications so far.

In this context, group III nitrides appear as the materials of choice to investigate CP physics at RT and polariton-based devices due to their larger E_X^B (~ 26 meV for bulk GaN layers and >40 meV in narrow QWs) (Ref. 6) and large coupling to the light field. Thus recently, the observation of SCR at RT was reported in a bulk GaN cavity through angular-resolved reflectivity experiments,⁸ and in an InGaIn/AlGaIn QW-MC by means of reflectivity and photoluminescence (PL) spectra measured at various exciton-photon detunings.^{9,10} Such preliminary results emphasize the potential of nitrides to explore RT CP phenomena but an in-depth understanding requires angular-resolved PL measurements. Indeed, these measurements are recognized as the main tool to probe CPs as they provide an access to in-plane dispersion curves and allow

determination of the CP population vs in-plane wavevector \mathbf{k}_{\parallel} .^{11,12} These types of measurements open the way to a large variety of physical phenomena, such as the determination of CP relaxation effects,¹² which is a prerequisite for the accurate development of nonlinear polariton devices.

In the present paper, we report a thorough RT study of the SCR in a hybrid bulk GaN MC with a bottom lattice-matched AlInN/AlGaIn distributed Bragg reflector (DBR), satisfying both high quality factor (Q) and narrow PL linewidth, by means of angle-resolved PL experiments. We show that the physics of strong coupling in GaN MCs differs significantly from their GaAs counterparts, namely that the symmetry of wurtzite semiconductors involves the coupling of the three free excitons X_A , X_B , and X_C to the cavity mode. We also discuss the oscillator strength values, the evolution of the polariton population vs angle for the lower polariton branch (LPB), and show that RT PL spectra exhibit a strong bottleneck effect.

The structure, grown by metalorganic vapor phase epitaxy on c -plane sapphire, consists of a standard $3\text{-}\mu\text{m}$ -thick GaN buffer layer, followed by a strain relieving layer, a 35 pair lattice-matched $\text{Al}_{0.85}\text{In}_{0.15}\text{N}/\text{Al}_{0.2}\text{Ga}_{0.8}\text{N}$ DBR, and a bulk $3\lambda/2$ GaN cavity ($\lambda \approx 360$ nm). The structure was then completed by the deposition of a 10 pair $\text{SiO}_2/\text{Si}_3\text{N}_4$ DBR [see Fig. 1(a)]. The use as a low refractive index layer of $\text{Al}_{0.85}\text{In}_{0.15}\text{N}$ lattice-matched to $\text{Al}_{0.2}\text{Ga}_{0.8}\text{N}$ instead of a high aluminum content AlGaIn layer reduces the built-in tensile strain occurring during the growth, and prevents the formation of cracks and/or dislocations while offering a significant refractive index contrast to $\text{Al}_{0.2}\text{Ga}_{0.8}\text{N}$. Q values in excess of 800 have been measured on MCs using a similar approach, establishing the state of the art for nitride-based MCs.¹³ Angle resolved PL was carried out under weak excitation power density ($P \sim 30$ W cm^{-2}) in reflection geometry using the 244 nm line of a continuous wave Ar⁺ laser frequency doubling unit, collected with an angular resolution of $\sim 1^\circ$ by a UV fiber, and detected by a monochromator, charge-coupled device (CCD) combination. All the results reported hereafter were obtained at RT.

A typical PL spectrum measured on the half MC structure (i.e., without top DBR) is displayed in Fig. 1(b) and compared to that of a thick GaN buffer layer grown on c -plane sapphire substrate. Both spectra are characterized by a simi-

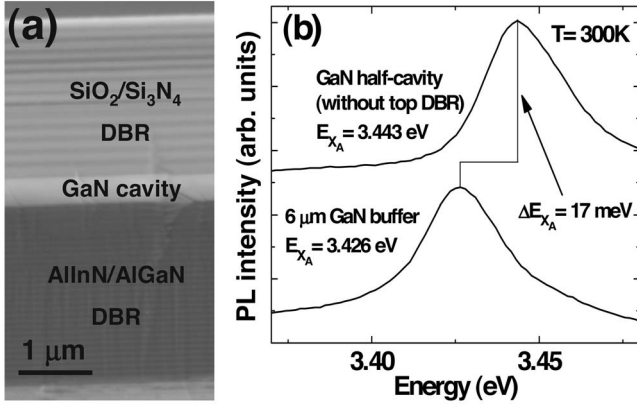


FIG. 1. (a) Scanning electron microscope image of the GaN cavity surrounded by an AlInN/AlGaIn bottom DBR and a SiO₂/Si₃N₄ top DBR. (b) RT PL spectrum of a relaxed GaN template layer grown on sapphire vs PL spectrum taken on the half-microcavity structure. The topmost spectrum has been upshifted for the sake of clarity.

lar full width at half maximum (~ 30 – 35 meV), close to the lowest value expected at RT. Note that a significant blueshift (~ 17 meV) of the main PL line, ascribed to the X_A free exciton, is observed between the half MC and the GaN epilayer, indicative of a compressive biaxial stress.¹⁴ This stress is likely to originate from a residual strain, which results from the underlying template and the bottom DBR. From this energy position, a compressive stress of 30 ± 5 kbar is deduced.¹⁴

TM and TE polarized PL spectra measured up to an angle $\theta = 36^\circ$ on the full MC structure using 2° steps are shown in Figs. 2(a) and 2(b), respectively. At first sight, two branches (bold lines) exhibiting an anticrossing are observed. An asymptotic approach toward the exciton X_A is visible for the lower PL line with increasing angles, while the second line stands above X_C . Such an anticrossing behavior can only be explained by considering a polariton picture. A detailed analysis of the PL spectra, i.e., by performing a careful deconvolution, reveals several branches, though not visible on

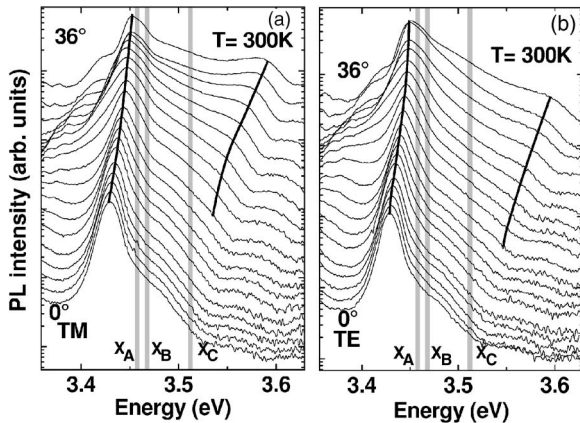


FIG. 2. (a) RT PL spectra as a function of angle for TM polarization. (b) Same as (a), but for TE polarization. Lines are a guide to the eye. The position of excitons is also quoted.

the whole range of angles except for the lower branch. Finally, the only way to account properly for these experimental observations requires the coupling of X_A , X_B , and X_C to the cavity mode.¹⁵

A marked difference is observed between TM and TE polarized PL spectra resulting from various contributions of optically active free excitons between both configurations. Indeed, the oscillator strength of excitons in wurtzite GaN is usually expressed with respect to σ and π polarizations, i.e., for cases where the electric field is either normal or parallel to the c axis of the crystal, respectively.¹⁴ Thus TE polarized spectra can be fully identified to σ polarization, while spectra measured under TM polarization correspond to a combination of σ and π polarizations. Then, knowing the compressive stress of the GaN layer, the relative oscillator strength and the energy of X_A , X_B , and X_C excitons can be determined.¹⁴ In our case, a weak and constant contribution is expected from X_C excitons in the TE case, whereas an increasing contribution is expected with increasing angles for TM polarization, which is effectively observed. In the subsequent analysis, we will focus on TE polarized spectra since a complete understanding of TM spectra would require an appropriate modeling of the contribution of σ and π polarizations, which is beyond the scope of this paper.

The experimental and fitted dispersion curves are reported on Fig. 3(a) for the TE case. The fitted curves were deduced from a 4×4 matrix Hamiltonian given by¹⁶

$$\begin{pmatrix} E_{cav} - j\Gamma_{cav} & V_{X_A} & V_{X_B} & V_{X_C} \\ V_{X_A} & E_{X_A} - j\Gamma_{X_A} & 0 & 0 \\ V_{X_B} & 0 & E_{X_B} - j\Gamma_{X_B} & 0 \\ V_{X_C} & 0 & 0 & E_{X_C} - j\Gamma_{X_C} \end{pmatrix}$$

where $E_{cav}(\theta=0^\circ)$ and Γ_{cav} are the bare cavity mode energy and half-width taken equal to 3.465 eV and 0.006 eV,¹⁷ respectively. The effective refractive index n_{eff} of the cavity, equal to 2.4, was deduced from the various refractive indices and the MC effective length.² The uncoupled exciton energies, E_{X_i} with $i=A, B$, and C , equal to 3.455, 3.465, and 3.512 eV, correspond to a compressive stress ~ 33 kbar. The exciton homogeneous broadenings, Γ_{X_i} , are taken equal to 0.013, 0.013 and 0.006 eV, respectively.¹⁸ The interaction potentials, V_{X_i} , deduced from the dispersion curves are equal to 0.025, 0.015, and 0.015 eV, respectively. Such values are 5 to 8 times larger than that encountered in GaAs (see e.g., Ref. 2). They differ also from those reported by Semond *et al.*⁸ as these authors considered a different approach where only X_A and X_B are coupled to the cavity mode, the contribution of X_C being not considered.

In Fig. 3(b), the relative fractions of the uncoupled modes, namely the squared modulus of the eigenstates, for each polariton mode are displayed vs θ . A significant contribution of several excitons is observed for the two middle polariton branches (MPB1 and MPB2), with a very small cavity component for MPB1 while the lower and upper polariton branches (LPB and UPB) are almost only the result of the mixing of the cavity mode and X_A (or X_C). Note that the accurate knowledge of exciton and photon fractions is cru-

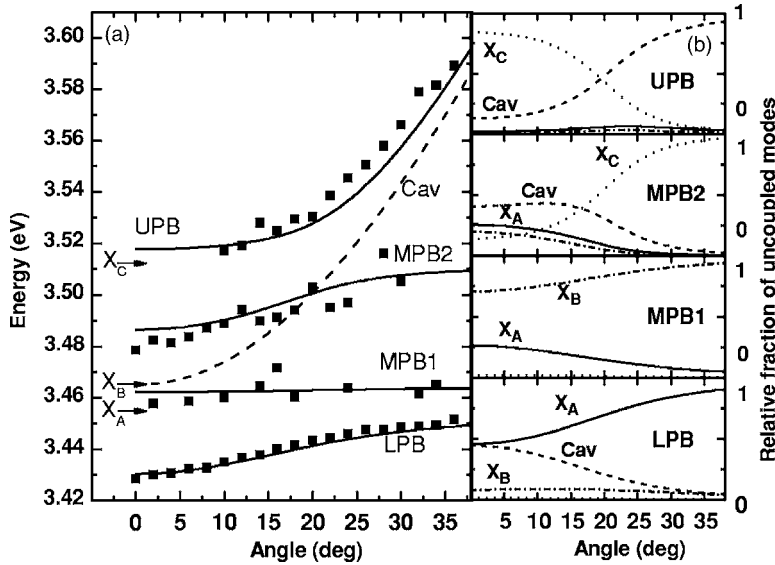


FIG. 3. Experimental energy positions vs θ together with calculated polariton dispersion curves (see text for details). The uncoupled modes are also reported. (b) Relative fractions of each of the uncoupled modes: cavity-photon C (---), X_A (—), X_B (---), and X_C (···) in the mixed polariton modes.

cial to investigate CP relaxation processes since it allows the determination of the polariton population along the dispersion curves.¹²

The oscillator strength of X_A , X_B , and X_C was deduced by modeling PL spectra in the TE case on the basis of the model described in Ref. 1, allowing us to calculate reflectivity (R) and transmission (T) coefficients of a Fabry-Perot cavity. The active region is modeled by a Lorentz oscillator

$$\epsilon(\omega) = \epsilon_b + \sum_{i=A}^C \frac{4\pi\alpha_{X_i}\omega_{X_i}^2}{\omega_{X_i}^2 - \omega^2 - 2j\Gamma_{X_i}\omega} \quad (1)$$

where ω is the pulsation of light, $\epsilon_b=6.9$ is the bulk cavity background dielectric function, α_{X_i} is the polarizability ($4\pi\alpha_{X_i}$ is also identified as the bulk exciton oscillator strength),¹⁹ and ω_{X_i} is the exciton pulsation. Finally, to account for the inhomogeneous broadening $\Gamma_{inh_{X_i}}$ of the excitonic transitions, a Gaussian distribution $g_{X_i}(\omega)$ was introduced for each oscillator with $\Gamma_{inh_{X_i}}=0.003, 0.003,$ and 0.07 eV for $X_A, X_B,$ and X_C , respectively.²⁰

Computed PL spectra were obtained assuming that PL spectra have a thermal line shape, i.e., they are well accounted for by the absorption spectrum ($A=1-R-T$) multiplied by a Boltzmann distribution, as shown in Ref. 21. A satisfactory fit (see Fig. 4) was obtained using oscillator strengths equal to $13 \times 10^{-3}, 12 \times 10^{-3},$ and 2×10^{-3} , respectively.²² This gives a relative strength for $X_A, X_B,$ and X_C excitons of 0.481, 0.445, and 0.074- $\sum_i 4\pi\alpha_{X_i}$ being normalized to unity. This is in very good agreement with values extrapolated from Fig. 3 in Ref. 14 for Γ_5 symmetry excitons for a GaN layer under a compressive biaxial stress of 33 kbar.

Note that in this analysis we did not consider a full non-local treatment of the dielectric function. Such a nontrivial approach, including spatial dispersion effects and appropriate boundary conditions, is still lacking for wurtzite GaN, where several excitons are involved. However, the right order of magnitude is obtained for the oscillator strengths as the esti-

mated value for X_A compares well with that previously reported for GaN epilayers.²⁰ These values are somewhat larger than those reported in Ref. 8, and are about one order of magnitude larger than that of GaAs.¹⁹ As such, these values open encouraging perspectives regarding the realization of nitride-based polariton devices.

To investigate further the apparently thermalized nature of the polariton emission, the evolution of the LPB population $N_{LPB}(\theta) \propto I_{PL}(\theta) \times \tau_{LPB}(\theta)$ with $I_{PL}(\theta)$ the integrated PL and $\tau_{LPB}(\theta)$ the radiative lifetime of the lower polariton state, inversely proportional to its photon fraction,¹² is reported in the inset of Fig. 4. $N_{LPB}(\theta)$ is compared to a quasithermal population proportional to $\exp[-E_{LPB}(\theta)/k_B T]$, where $E_{LPB}(\theta)$ is the energy of the lower polaritons along the dispersion curve. The significantly larger population measured at great angles with respect to small ones demonstrates the

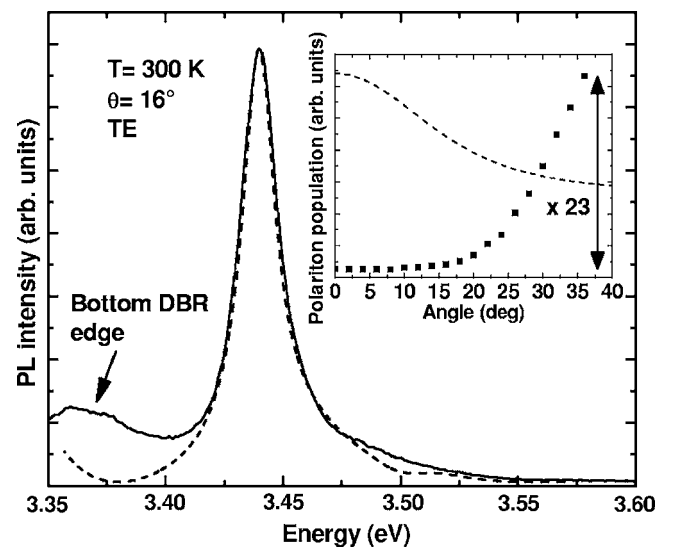


FIG. 4. Experimental PL spectrum measured at $\theta=16^\circ$ (—) and the corresponding calculated spectrum (---). Inset: Experimental polariton population of the LPB (■) and calculated one considering a thermalized population (---).

presence of a polariton relaxation bottleneck.^{12,23} This behavior differs strikingly from the calculated population and illustrates the inefficiency of the relaxation rates—occurring mainly through acoustic phonons and structural disorder—as compared to the radiative recombination rates. Similar, and more detailed, studies at various detunings could be extended to nitride-based QW-MCs as the situation might reveal different results. Such investigations are of importance as the search for dynamical polariton condensates and the future polariton-based devices are likely to rely on QW heterostructures.

In conclusion, strong exciton-photon coupling between the three optically active bulk GaN excitons and the cavity mode in a bulk GaN MC has been reported at RT by means of angular-resolved PL measurements. Parameters such as

the bulk exciton oscillator strength and bare mode fractions of the polariton mixed modes have been estimated. Polariton luminescence is shown to exhibit a strong bottleneck effect despite its thermal line shape. RT polariton emission in GaN MCs represents a significant step in polariton physics as it should make possible the development of polariton-based devices.

The authors thank V. Savona for fruitful discussions and R. Houdré for a critical reading of the manuscript. This work was carried out in the framework of the NCCR Quantum Photonics program of the Swiss National Science Foundation. N. G. and R. B. are indebted to Sandoz Family Foundation for its financial support.

¹C. Weisbuch, M. Nishioka, A. Ishikawa, and Y. Arakawa, Phys. Rev. Lett. **69**, 3314 (1992).

²For a review see, e.g., M. S. Skolnick, T. A. Fisher, and D. M. Whittaker, Semicond. Sci. Technol. **13**, 645 (1998).

³A. Tredicucci, Y. Chen, V. Pellegrini, M. Börger, L. Sorba, F. Beltram, and F. Bassani, Phys. Rev. Lett. **75**, 3906 (1995).

⁴P. G. Savvidis, J. J. Baumberg, R. M. Stevenson, M. S. Skolnick, D. M. Whittaker, and J. S. Roberts, Phys. Rev. Lett. **84**, 1547 (2000).

⁵A. Imamoğlu, R. J. Ram, S. Pau, and Y. Yamamoto, Phys. Rev. A **53**, 4250 (1996).

⁶G. Malpuech, A. di Carlo, A. V. Kavokin, J. J. Baumberg, A. Zamfirescu, and P. Lugli, Appl. Phys. Lett. **81**, 412 (2002).

⁷M. Saba, C. Ciuti, J. Bloch, V. Thierry-Mieg, R. André, Le Si Dang, S. Kundermann, A. Mura, G. Bongiovanni, J. L. Staehli, and B. Deveaud, Nature (London) **414**, 731 (2001).

⁸F. Semond, I. R. Sellers, F. Natali, D. Byrne, M. Leroux, J. Massies, N. Ollier, J. Leymarie, P. Disseix, and A. Vasson, Appl. Phys. Lett. **87**, 021102 (2005).

⁹T. Tawara, H. Gotoh, T. Akasaka, N. Kobayashi, and T. Saitoh, Phys. Rev. Lett. **92**, 256402 (2004).

¹⁰T. Tawara, H. Gotoh, T. Akasaka, N. Kobayashi, T. Makimoto, and T. Saitoh, Phys. Status Solidi C **2**, 809 (2005).

¹¹The angle θ , measured from the normal to the sample, is linked to \mathbf{k}_{\parallel} through the relationship $|\mathbf{k}_{\parallel}| = \omega/c \sin \theta$.

¹²A. I. Tartakovskii, M. Emam-Ismael, R. M. Stevenson, M. S. Skolnick, V. N. Astratov, D. M. Whittaker, J. J. Baumberg, and J. S. Roberts, Phys. Rev. B **62**, R2283 (2000).

¹³E. Feltin, R. Butté, J.-F. Carlin, J. Dorsaz, N. Grandjean, and M. Illegems, Electron. Lett. **41**, 94 (2005).

¹⁴B. Gil and O. Briot, Phys. Rev. B **55**, 2530 (1997).

¹⁵The spectral features visible below the lower bold line and above the upper bold line correspond to regions emitting out of the

bottom DBR stopband, i.e., they are not linked to polariton emission.

¹⁶In our analysis, the influence of the continuum is neglected which leads to interaction potentials V_{X_i} independent of \mathbf{k}_{\parallel} . This approach is justified *a posteriori* when considering experimental results though we cannot completely exclude some effects on X_C .

¹⁷Neglecting the contribution of X_B and X_C , the linewidth of the LPB can be roughly considered as equally shared between the homogeneous broadening of X_A and the cavity mode at $\theta=0^\circ$, the situation where the uncoupled modes are the closer, which leads to $\Gamma_{cav}=6$ meV.

¹⁸The lower value of Γ_{X_C} is explained by its lower oscillator strength, as shown below. Note that up to $\Gamma_{X_i} \approx 25$ meV, there is hardly any change between dispersion curves calculated with and without damping.

¹⁹Y. Chen, A. Tredicucci, and F. Bassani, Phys. Rev. B **52**, 1800 (1995).

²⁰The larger value of $\Gamma_{inh_{X_C}}$ is explained by the larger sensitivity of X_C to strain fluctuations. It is taken to be equal to the ratio of the slope of E_{X_C} vs biaxial stress with that of E_{X_A} times $\Gamma_{inh_{X_A}}$. See, e.g., M. Tchounkeu, O. Briot, B. Gil, J. P. Alexis, and R.-L. Aulombard, J. Appl. Phys. **80**, 5352 (1996).

²¹R. P. Stanley, R. Houdré, C. Weisbuch, U. Oesterle, and M. Illegems, Phys. Rev. B **53**, 10995 (1996).

²²The slight discrepancy observed between theory and experiment for the upper part of the PL spectrum might be explained by the absence of nonresonant band to band light absorption in our linear dispersion model.

²³See V. Savona, in *Confined Photon Systems, Fundamentals and Applications*, edited by H. Benisty, J.-M. Gérard, R. Houdré, J. Rarity, and C. Weisbuch (Springer, Berlin, 1999), p. 225.